

## Article

# Parametric Mathematical Model of the Electrochemical Degradation of 2-Chlorophenol in a Flow-by Reactor under Batch Recirculation Mode

Alejandro Regalado-Méndez <sup>1,\*</sup>, Guadalupe Ramos-Hernández <sup>1</sup>, Reyna Natividad <sup>2</sup>, Mario E. Cordero <sup>3</sup>, Luis Zárate <sup>3</sup>, Edson E. Robles-Gómez <sup>1</sup>, Hugo Pérez-Pastenes <sup>4</sup> and Ever Peralta-Reyes <sup>1,\*</sup>

- <sup>1</sup> Research Laboratories, Universidad del Mar-Campus Puerto Ángel, Puerto Ángel 70902, Oaxaca, Mexico; a.123.grhfm1.123@gmail.com (G.R.-H.); edson\_robles@aulavirtual.umar.mx (E.E.R.-G.)
- <sup>2</sup> Chemical Engineering Laboratory, Centro Conjunto de Investigación en Química Sustentable, UAEM-UNAM, Universidad Autónoma del Estado de México, Toluca 50200, Estado de México, Mexico; reynanr@gmail.com
- <sup>3</sup> Escuela de Ingeniería Química, Universidad Popular Autónoma del Estado de Puebla, Puebla 72410, Puebla, Mexico; marioedgar.cordero@upaep.mx (M.E.C.); luis.zarate@upaep.mx (L.Z.)
- <sup>4</sup> Facultad de Ciencias Químicas, Universidad Veracruzana-Campus Coatzacoalcos, Coatzacoalcos 96538, Veracruz, Mexico; huperez@uv.mx
- \* Correspondence: alejandro.regalado33@gmail.com (A.R.-M.); e\_pere70@hotmail.com (E.P.-R.); Tel.: +52-958-1079861 (A.R.-M.); +52-958-5890618 (E.P.-R.)

**Abstract:** 2-Chlorophenol (2-CP) is a dangerous organic contaminant found in wastewater. In this work, 2.5 L of a 2-CP solution (1 mol/m<sup>3</sup>) was electrochemically treated in a flow-by reactor equipped with two boron-doped diamond electrodes (BDD) under batch recirculation mode for a period of 4 h, a current density of 0.14 A/cm<sup>2</sup>, a volumetric flow rate of 1 L/min, and pH = 7.3. In this work, a parametric mathematical model of the degradation efficiency of 2-CP was developed using an axial dispersion model and a continuous stirred tank for the flow-by reactor (FBR), which was constructed using a shell mass balance considering the dispersion and convection terms and the reservoir tank (CST), which was constructed using a mass balance of 2-CP. The parametric mathematic model of the electrochemical degradation of 2-chlorophenol was numerically resolved by employing the software package COMSOL Multiphysics<sup>®</sup> V. 5.3, where a mass transfer equation for diluted species and a global differential equation represents the FBR and CST, respectively. The results indicate that the parametric mathematical model proposed in this research fits the experimental results, and this is supported by the index performance values such as the determination coefficient ( $R^2 = 0.9831$ ), the mean square error (MSE = 0.0307), and the reduced root-mean-square error (RMSE = 0.1754). Moreover, the degradation efficiency of 2-CP estimated by the proposed model achieves 99.06%, whereas the experimental degradation efficiency reached 99.99%, a comparative error of 0.93%. This corroborates the predictive ability of the developed mathematical model and the effectiveness of the employed electrooxidation process. Finally, a 0.143 USD/L total operating cost for the electrochemical plant was estimated.

**Keywords:** 2-chlorophenol; electrochemical degradation; parametric mathematical model; flow-by reactor



**Citation:** Regalado-Méndez, A.; Ramos-Hernández, G.; Natividad, R.; Cordero, M.E.; Zárate, L.; Robles-Gómez, E.E.; Pérez-Pastenes, H.; Peralta-Reyes, E. Parametric Mathematical Model of the Electrochemical Degradation of 2-Chlorophenol in a Flow-by Reactor under Batch Recirculation Mode. *Water* **2023**, *15*, 4276. <https://doi.org/10.3390/w15244276>

Academic Editor: Sergi Garcia-Segura

Received: 30 October 2023

Revised: 25 November 2023

Accepted: 12 December 2023

Published: 14 December 2023

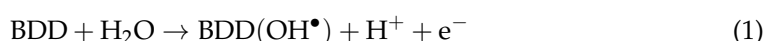


**Copyright:** © 2023 by the authors. Licensee MDPI, Basel, Switzerland. This article is an open access article distributed under the terms and conditions of the Creative Commons Attribution (CC BY) license (<https://creativecommons.org/licenses/by/4.0/>).

## 1. Introduction

Chlorophenols (e.g., 4-chlorophenol, 2-chlorophenol (2-CP), and 2,4-dichlorophenol, among others) are recognized worldwide as some of the most dangerous organic contaminants [1] in wastewater because of their high toxicity, carcinogenicity, and resistance to biodegradation [2]. Common sources of phenolic compounds in bodies of water are paints, polymeric resins, petrochemical industries, pesticides, and health products [3]. Because of their negative effect on human health and the environment, these contaminants must be eliminated from wastewater [4]. Among the available technologies for wastewater

treatment (physicochemical [5], chemical [6], biological (removal efficiency of 89%) [7], and advanced oxidation processes (AOPs, [8])), the electrooxidation processes emerge as a sophisticated and environmentally amicable tool. In this context, different anodic electrodes such as those made from Pt, PbO<sub>2</sub>, SnO<sub>2</sub>, DSA (e.g., Ta<sub>2</sub>O<sub>5</sub>-IrO<sub>2</sub> and Nb<sub>2</sub>O<sub>5</sub>-IrO<sub>2</sub>), and BDD have been employed in many electrooxidation processes. The Pt electrode is expensive and has low oxidation efficiency, the PbO<sub>2</sub> electrode is susceptible to corrosion and dangerous for health and the environment, the SnO<sub>2</sub> electrode is cheap and has a low degradation rate, the DSA electrodes are not stable enough over an extended period, and the boron-doped diamond (BDD) electrode is stable for a long time and has high degradation efficiencies in comparison with all the electrodes mentioned above [9]. The high degradation efficiency of BDD electrodes is due to the generation of hydroxyl radicals (OH•) [10] that proceeds on the anode surface according to Equation (1) [11]. Additionally, OH• (oxidation potential of 2.8 V) is second on the list of the twelve principal oxidant species [12],



The employment of BDD electrodes upgrades the electrochemical treatments as cutting-edge technology since this has been successfully used for the degradation and mineralization of an immense number of organic compounds, such as phenolic pollutants, drugs, dyes, and others [13]. The application of this technology, however, has been mostly assessed at the laboratory and pilot scales. To advance further in the scaling-up process, i.e., the industrial dimension, mathematical models are key. In this sense, the available literature reports on the modeling of flow-by-reactor hydrodynamics assume laminar ([14]) or turbulent ([15]) flow patterns.

The literature on the experimental electrochemical degradation of organic compounds (e.g., chlorophenols) is abundant, whereas the theoretical modeling of the electrolysis of organic compounds in FBRs is sufficient to understand the state-of-art models of electrolysis processes such as those revealed in reference [16]. However, the literature on the complete modeling of the electrochemical degradation process of persistent organic compounds and their validation is scarce. Based on a literature review, the development and solution of 3D models for FBRs that incorporate hydrodynamics, mass transport, current and potential distribution, and reaction rate kinetics is a very complex because the effects of mass transport and local velocities cannot be computed simply. Therefore, the mathematical parametric models allow us to quantify those values in a relatively easy way. Additionally, these models consider only one direction, convection, and axial dispersion terms as mass transport at a transient state. One advantage of this parametric model lies in the axial dispersion coefficient that can be obtained experimentally by a retention time distribution (RTD) analysis [17].

Table 1 summarizes the scientific works we found on the complete modeling of electrochemical plants conducted in FBRs. In this table, the operating conditions for various electrochemical processes are presented. Additionally, different flow-by reactor configurations are depicted, where the main differences between all reactor configurations are the flow inlet and outlet and turbulence promoters (are used or not). For instance, the flow-by reactor employed in reference [18] does not have turbulence promoters and the flow direction is an “S”-curve shape that is unlike the other FBR configurations (“C”-curve shape) displayed in Table 1. Additionally, the procedure to solve the different models is summarized in Table 1.

In references [14,19–21], the authors only consider FBRs in electrochemical wastewater treatment, whereas in references [18,22,23] the authors consider an FBR and a continuous stirred tank (CST) as the electrochemical wastewater treatment in a batch recirculation regimen. This is given because the solution of rigorous mathematical models for an FBR coupled with a CST in the transitory state for the electrochemical degradation of organic compounds requires a lot of computer time to solve the set of partial differential equations (PDEs) generated (continuity, momentum, mass transport, and potential distribution equations). Therefore, this type of set of equations is relatively difficult to solve since

the numerical solution of the PDEs of the FBR model coupled with the EDO of the CST is complicated because of the length scales, different times, and concentration changes of the chemical species concerning the chemical potential in the solution. These factors cause a considerable increase in the computational requirements and, as a result, these phenomenological mathematical models are converted to a numerical problem. Thus, the parametric mathematical models (PMMs) emerge as a very good tool for developing the mathematical models of electrochemical plants for the electrochemical degradation of persistent organic compounds because the computer time is reduced considerably and the solution of the PMMs is easier. The electrooxidation takes place on the anode surface. The electrochemical reaction rate can be modeled by a pseudo-homogeneous kinetic equation.

It is worth pointing out that the procedure to solve the model of reference [18] consists of two steps; the first one solves the set of continuity and mass transport equations in the COMSOL Multiphysics @ 5.3 software and the second one solves the stirred-tank equation in the MATLAB @ 2017a software via a LiveLink between both software platforms. This procedure spent 42 days of computing time for the 4 h of electrochemical reaction time. This work presents and discusses a different procedure to solve the proposed model in significantly less computing time.

**Table 1.** Existing literature on modeling of electrochemical processes carried out in an FBR.

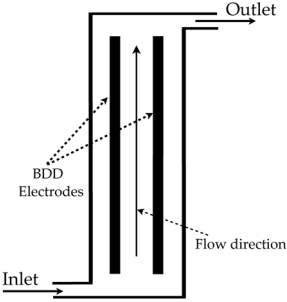
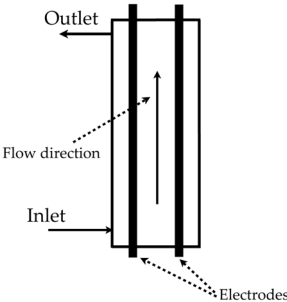
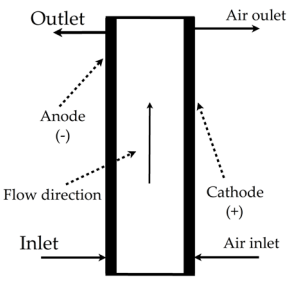
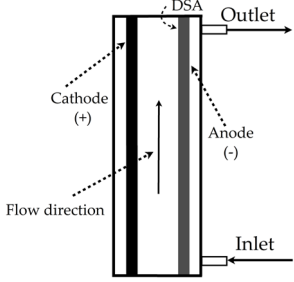
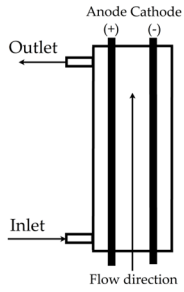
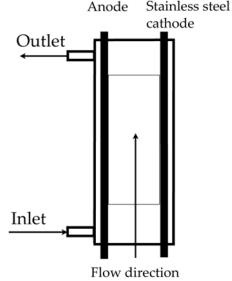
Process	Reactor Configuration	Environmental Conditions	Solution Via	Ref.
Electrooxidation of 2-CP		Hydroxyl radicals, volumetric flow rate of 1.0 L/min, pH of 3, volume treated of 2.5 L, current density of 140 mA/cm <sup>2</sup> , 0.1 mol/L of Na <sub>2</sub> SO <sub>4</sub> , D <sub>ax</sub> of 0.0005 m <sup>2</sup> /s, temperature of 25 °C	Software COMSOL Multiphysics® 5.3/Win64 interacting with the software MATLAB® 2017a	[18]
Electrochemical oxidation of crystal violet dye		Hydroxyl radical, pH of 6.4, currents density of 10 mA/cm <sup>2</sup> , 0.25 mol/L of Na <sub>2</sub> SO <sub>4</sub> , D <sub>ax</sub> of 0.00042 m <sup>2</sup> /s, volumetric flow rate of 3 L/min, temperature of 25 °C	Software FlexPDE academic version 6.36/W32	[22]
Electro-peroxone degradation of orange reactive 16-dye		Hydrogen peroxide, pH of 3, volumetric flow rate of 1.135 L/min, D <sub>ax</sub> of 0.00153 m <sup>2</sup> /s, volume treated of 2 L, current density of 10 mA/cm <sup>2</sup> , 0.05 mol/L of Na <sub>2</sub> SO <sub>4</sub> , and 0.5 L/min of O <sub>3</sub> , temperature of 25 °C	Software COMSOL Multiphysics® 5.3/Win64	[20]

Table 1. Cont.

Process	Reactor Configuration	Environmental Conditions	Solution Via	Ref.
Sulfamethoxazole degradation		Active chlorine (HOCl), current density of 10 mA/cm <sup>2</sup> , 0.02 mol/L of NaCl, volumetric flow rate of 5 L/min, temperature of 25 °C	Software COMSOL Multiphysics® 5.2a commercial	[19]
Indigo carmine dye		Active chlorine (HOCl), 0.05 mol/L of NaCl, volumetric flow rate of 0.9 L/min, current density of 200 mA/cm <sup>2</sup> , temperature of 25 °C	Software FlexPDE professional version 6.5/W64 3D	[23]
Reactive Black 5		Active chlorine (HOCl), 0.05 mol/L of NaCl, volumetric flow rate of 0.8 L/min, current density of 200 mA/cm <sup>2</sup> , temperature of 25 °C	Software COMSOL Mul-tiphysics®	[14]

In this work, a parametric mathematical model of the electrochemical degradation efficiency of 2-CP in a complete electrolysis system (electrochemical plant) was developed using an axial dispersion model (model of the flow-by reactor (FBR)) coupled with a recirculation tank (model of the continuous stirred tank (CST)). This model was solved numerically via the commercial software package COMSOL Multiphysics® V. 5.3, where the complete electrochemical plant is represented by a mass transfer equation for diluted species for the FBR and a global differential equation (EDOs and EDAs) for the CST that is coupled to the FBR. Additionally, this research intends to generate a better comprehension of the complete mathematical models of electrochemical plant treatments for wastewater that contains persistent organic compounds (e.g., 2-chlorophenol) through experimental validation.

## 2. Materials and Methods

### 2.1. System Description

The electrochemical degradation of 2-CP was performed in an FBR with a total length of 23.4 cm, a width of 4.8 cm, an effective length of 20 cm, a channel thickness of 0.5 cm, a  $V_T$  of 3.5 L, and that is equipped with two BDD electrodes ( $\ell = 20$  cm). More detail about the FBR can be found in the author's previous work [24]. The experimental system for the electrochemical degradation of 2-CP was comprised an FBR coupled to a polycarbonate reservoir tank (CST). The synthetic wastewater was supplied into the FBR by using a magnetic pump at 300 rpm, where the volumetric flow rate was controlled using a glass rotameter, the pipeline, valves, and connectors were made from PVC, and a power supply

was employed to energize the electrodes. Figure 1 shows the flow chart of the complete electrochemical plant.

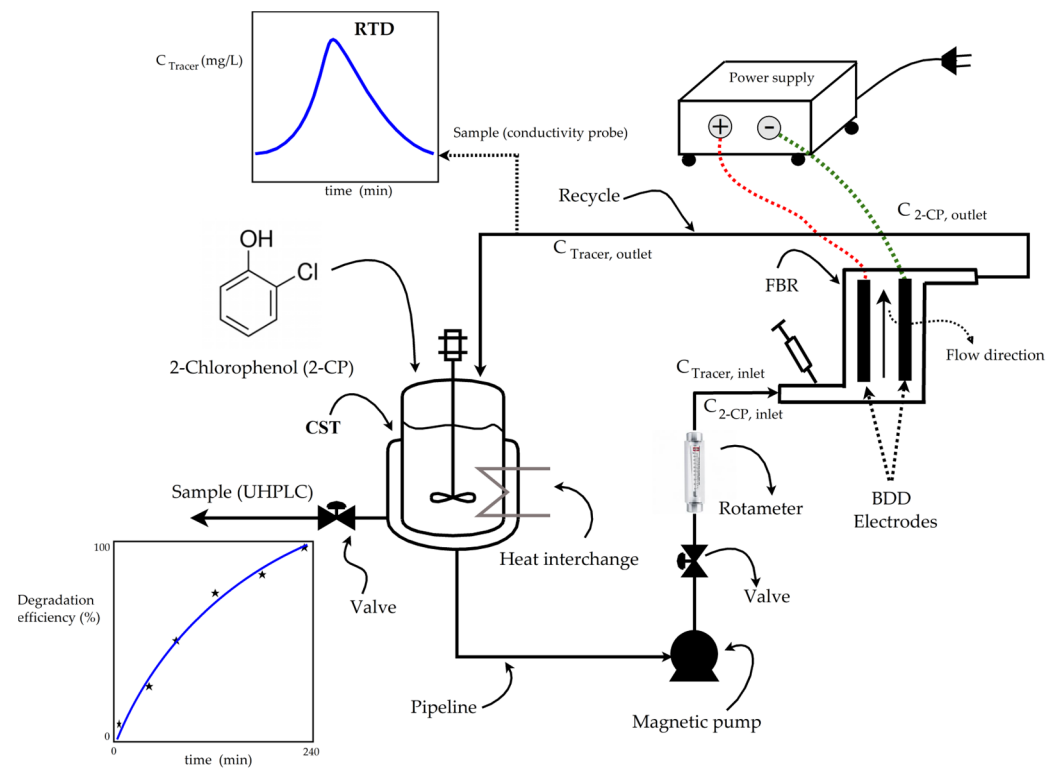


**Figure 1.** Electrochemical plant diagram.

## 2.2. RTD Analysis

A saturated solution of NaCl was employed as a tracer to visualize the flow pattern of the FBR depicted in Figure 1. A total of 10 mL of tracer solution was manually injected with a syringe into the inlet of the FBR for the experiment at a volumetric flow rate of 1.0 L/min. The liquid conductivity at the FBR outlet was measured by using a Vernier® Conductivity Probe every 0.33 s until the conductivity measurement was zero. Additionally, the RTD experiment was performed in triplicate and the calibration curve between the concentration (mg/L) and conductivity ( $\mu\text{S}/\text{cm}$ ) was obtained.

## 2.3. Electrolysis of 2-CP

The procedure to conduct the electrochemical degradation of 2-CP and the determination of 2-CP at different times was similar to that reported in reference [25], where the operation conditions were a volumetric flow rate of 1.0 L/min, an initial pH of 7.3, an electric current density of  $0.14 \text{ A}/\text{cm}^2$ , and a reaction time of 4 h.

## 2.4. Parametric Mathematical Model and Solution Method

As with all good mathematical models, some considerations are necessary to understand the scope of the developed model. In the case of this study, the model was developed assuming the following basic considerations:

- The reservoir tank was simulated using a CST.
- The boundaries of the FBR inlet and outlet were both of the closed–closed vessel type [17].
- The electrooxidation of 2-CP took place on the electrode surface at a constant current.
- The hydroxyl radicals were uniformly formed on the surface of the electrode [26]. Hence, the reaction rate of 2-CP was modeled using a pseudo-first order.
- The FBR was isothermally operated.

- The electrooxidation of 2-CP was limited by the mass transfer of 2-CP from the bulk to the electrode surface [18].

#### 2.4.1. Axial Dispersion Mathematical Model for the Flow-By Reactor

In this investigation, a partial differential equation for the axial dispersion mathematical (ADM) model (see Equation (2)) with closed–closed vessel boundary conditions ([27], Equations (3) and (4)) and initial condition (Equation (5)) was employed to represent the FBR, since it has been reported that a large number of FBRs have a similar plug-flow flow pattern, which is in agreement with [24] for the same electrochemical reactor. The ADM model considers the deviations from the ideal plug-flow reactor by introducing the dispersion term [17]. The procedure to obtain Equation (2) can be found in Appendix A.

$$\overbrace{\frac{\partial C_{2-CP}^{FBR}}{\partial t}}^{\text{Acumulation}} = \underbrace{D_{ax} \frac{\partial^2 C_{2-CP}^{FBR}}{\partial x^2}}_{\text{Difussion transport}} - \underbrace{u \frac{\partial C_{2-CP}^{FBR}}{\partial x}}_{\text{Convection transport}} + \underbrace{r_{2-CP}}_{\text{Is zero when there is no reaction}} \quad (2)$$

Considering a perfect mixing at the inlet and the outlet of the FBR [15], Equation (3) represents the fact that the flow rate of the 2-CP being fed to the FBR is equal to the diffusion term at  $x = 0$ . Equation (4) describes that the mass flux of the 2-CP at the outlet ( $x = \ell$ ) of the FBR is set to zero ( $N_{2-CP} = 0$  or  $-D_{ax} \frac{\partial^2 C_{2-CP}^{FBR}}{\partial x^2} = 0$ ). In addition, Equation (5) indicates the initial condition, which represents the initial concentration of the 2-CP ( $C_{2-CP,0} = 1 \text{ mol/m}^3$ ) at  $t = 0$ .

$$\text{At } x = 0 \quad D_{ax} \frac{\partial^2 C_{2-CP}^{FBR}}{\partial x^2} = u \cdot C_{2-CP,0} \quad \forall t > 0 \quad (3)$$

$$\text{At } x = \ell \quad -D_{ax} \frac{\partial^2 C_{2-CP}^{FBR}}{\partial x^2} = 0 \quad \forall t > 0 \quad (4)$$

$$\text{At } t = 0 \quad C_{2-CP}^{FBR} = C_{2-CP,0} \quad \forall 0 < x < \ell \quad (5)$$

where  $C_{2-CP}^{FBR}$  ( $\text{mol/m}^3$ ) is the local concentration of 2-CP at any time that feeds the CST,  $D_{ax}$  is the axial dispersion coefficient ( $\text{m}^2/\text{s}$ ),  $x$  is the FBR length (cm),  $u(\partial C_{2-CP}^{FBR} / \partial x)$  is the convection transport term,  $D_{ax}(\partial^2 C_{2-CP}^{FBR} / \partial x^2)$  is the dispersion transport term,  $r_{2-CP}$  is the reaction rate of 2-CP ( $\text{mol/h}$ ), and  $k_{app}$  is the apparent first-order reaction rate constant ( $1/\text{h}$ ).

$$r_{2-CP} = -\underbrace{k_{OH} C_{2-CP}^{FBR}}_{k_{app}} = -k_{app} C_{2-CP}^{FBR} \quad (6)$$

For this work, the reaction kinetics were pseudo-first order, as reported in [11], and are given by Equation (6), where the electrochemical degradation of 2-CP was performed at a  $\text{pH}_0$  of 7.3, a current density of  $0.14 \text{ A/cm}^2$ , and a volumetric flow rate of  $1.0 \text{ L/min}$  within 4 h of electrolysis time. Additionally, the axial dispersion coefficient ( $D_{ax}$ ) was calculated according to [24]. The  $D_{ax}$  was computed when the FBR operates at a linear velocity of  $0.0947 \text{ m/s}$ , a volumetric flowrate of  $1 \text{ L/min}$ , a Reynolds number of  $21,208.73$ , and a Peclet number of  $39.93$ .

#### 2.4.2. Continuous Stirred Tank (CST) Model for the Reservoir Tank

The mass balance for the reservoir tank is represented by Equation (7). A complementary expression that solves this mass balance is given by Equation (8). The derivation of Equation (7) can be found in Appendix A.

$$\frac{dC_{2-CP}^{CST}}{dt} = \frac{Q}{V_T} (C_{2-CP}^{FBR} - C_{2-CP}^{CST}) \quad (7)$$

$$\text{At } t = 0 \text{ } C_{2\text{-CP}}^{\text{CST}} = C_{2\text{-CP},0} \quad (8)$$

where  $C_{2\text{-CP}}^{\text{CST}}$  (mol/m<sup>3</sup>) is the outlet concentration of 2-CP from the CST that feeds the FBR,  $V_T$  is the reservoir tank volume (L),  $Q$  is the volumetric flow rate (L/min), and  $t$  is the electrolysis time (min).

#### 2.4.3. Numerical Solution Approach

The numerical solution strategy to solve the parametric mathematical model of the electrochemical degradation of 2-chlorophenol in the FBR under batch recirculation mode was conducted as follows: the solution of the model given by the set of the Equations (2)–(8) was achieved numerically via the commercial software package COMSOL Multiphysics<sup>®</sup> 5.3/win64, where the mass balance of the FBR (Equation (2)) was represented in the software by the mass transfer equation for diluted species and the mass balance of the CST (Equation (7)) was represented in the commercial software by a global differential equation (EDOs and EDAs). The numerical method to resolve the partial differential equation and the ordinary differential equation was the finite element, where the simulation mesh domain was controlled by the physics, the length of the elements was marked as normal, and the desired accuracy was  $1 \times 10^{-5}$ .

Upon implementing the model in the mentioned software package, the simulation was conducted in macOS Catalina version 10.15.7 (19H2026) using an iMac (27-inch, late 2013) equipped with an Intel<sup>®</sup> Core i5 processor at 3.2 GHz with four nucleus and 16 GB of RAM.

Finally, the degradation efficiency variable (see Equation (9)) was employed for the visualization of the results of the model of the electrochemical degradation of 2-CP.

$$\eta = \left( \frac{C_{2\text{-CP},0} - C_{2\text{-CP}}|_t}{C_{2\text{-CP},0}} \right) \times 100 \quad (9)$$

where  $\eta$  is the degradation efficiency of 2-CP,  $C_{2\text{-CP},0}$  (mol/m<sup>3</sup>) is the outlet concentration of 2-CP, and  $C_{2\text{-CP}}|_t$  (mol/m<sup>3</sup>) is the concentration of the 2-CP at any time.

#### 2.4.4. Performance of the Model

The accuracy precision of the model developed regarding the experimental data was judged by the classic error metrics such as the root-mean-square error (RMSE, [28], see Equation (10)) and mean square error (MSE [29], see Equation (11)). The RMSE and MSE assume that the ensuing errors are impartial and follow a normal distribution [30]. For all error metrics, a low value is desirable.

$$RMSE = \sqrt{\frac{1}{n} \sum_{i=1}^n \left( \frac{\eta_{exp,i}^2 - \eta_{model,i}^2}{\eta_{exp}^2} \right)^2} \quad (10)$$

$$MSE = \frac{1}{n} \sum_{i=1}^n (\eta_{exp,i} - \eta_{model,i})^2 \quad (11)$$

where  $n$  is the number of data points,  $\eta_{exp}$  is the experimental degradation efficiency of 2-CP, and  $\eta_{model}$  is the modeled degradation efficiency of 2-CP.

#### 2.4.5. Energy Balance and Total Operating Cost

The total operating cost was calculated as a function of the electricity and electrolyte price (see Equation (16)). The electricity price includes the electricity used by the electrodes, the electricity used by the recirculation pump, and the electricity used by the heat interchange pump. Hence, the total electrical energy consumption (EC (kW h)) for the

electrochemical plant, especially for the electrochemical degradation of 2-CP, was computed by the set of Equations (12)–(15).

$$E_{electrodes} = U \times j \times A \times t \quad (12)$$

$$E_{pump, flow} = P_n \times t \quad (13)$$

$$E_{pump, heat interchanger} = P_m \times t \quad (14)$$

$$EC = E_{Electrodes} + E_{pump, flow} + E_{pump, heat interchanger} \quad (15)$$

$$Cost = \alpha EC + \beta m_{electrolyte} \quad (16)$$

where  $EC$  is the total energy consumption (kW h),  $U$  is the average cell potential (25.16 V),  $A$  is the total surface area (32 cm<sup>2</sup>),  $j$  is the applied current density (A/cm<sup>2</sup>),  $t$  is the reaction time (h),  $E_{electrodes}$  is the electricity used by the electrodes (kW h),  $E_{pump,flow}$  is the electricity used by the recirculation pump,  $E_{pump,heat}$  exchanger is the electricity used by the heat exchanger pump,  $P_n$  is the supplier catalog nominal power (0.198 kW) for the recirculation pump,  $P_m$  is the supplier catalog nominal power (0.123 kW) for the heat interchanger pump,  $Cost$  is the total operating cost (USD),  $\alpha$  is the electricity price (0.046 USD/kW h, based on 1 USD/MXN 18.32),  $\beta$  is the price of the electrolyte (0.8 USD/kg), and  $m_{electrolyte}$  is the consumed electrolyte mass (kg).

### 3. Results and Discussions

#### 3.1. ADM Validation

According to Section 2.2, the calibration curve to convert the electrical conductivity ( $\mu\text{S}/\text{cm}$ ) to tracer concentration (mg/L) has a linear relationship ( $m = 0.5694$  mg cm/L  $\mu\text{S}$ ) with a correlation coefficient ( $R^2$ ) of 0.9925.

To verify that the ADM model fits the experimental data given by an RTD analysis, a Gaussian pulse function (see Equation (17)) was employed and substituted as an initial condition similar that in [15]. Additionally, the ADM model was solved via the finite element method employing COMSOL<sup>®</sup> 5.3/win64.

$$C(t) = \frac{\exp\left(-\frac{(t-t_m)^2}{2\sigma^2}\right)}{\sigma\sqrt{2\pi}} \quad (17)$$

where  $t$  is time,  $\sigma^2$  is standard deviation, and  $t_m$  is mean residence time in the FBR.

The mean residence time ( $t_m = 12.23$  s) was computed using Equation (18) and the standard deviation ( $\sigma^2 = 7.29$  s<sup>2</sup>) was computed by applying Equations (19) and (20) according to [31].

$$t_m = \frac{\int_0^\infty tCdt}{\int_0^\infty Cdt} \cong \frac{\sum_i t_i \bar{C}_i}{\sum_i \bar{C}_i} \quad (18)$$

$$E(t) = \frac{C(t)}{\int_0^\infty C(t)dt} \cong \frac{C(t)}{C_0} \quad (19)$$

$$\sigma^2 = \int_0^\infty (t - t_m)E(t)dt \quad (20)$$

In Figure 2, the comparison between the RTD analysis and the simulation of the FBR is shown. The blue shape depicted in Figure 1 fits very well the experimental data (star points). Therefore, the shape curve and experimental data suggest a plug-flow pattern in



concordance with reference [24]. Hence, the ADM model described by Equations (2)–(5) when there is no reaction term ( $r_{2-CP} = 0$ ) can be used to model the hydrodynamics of the FBR.

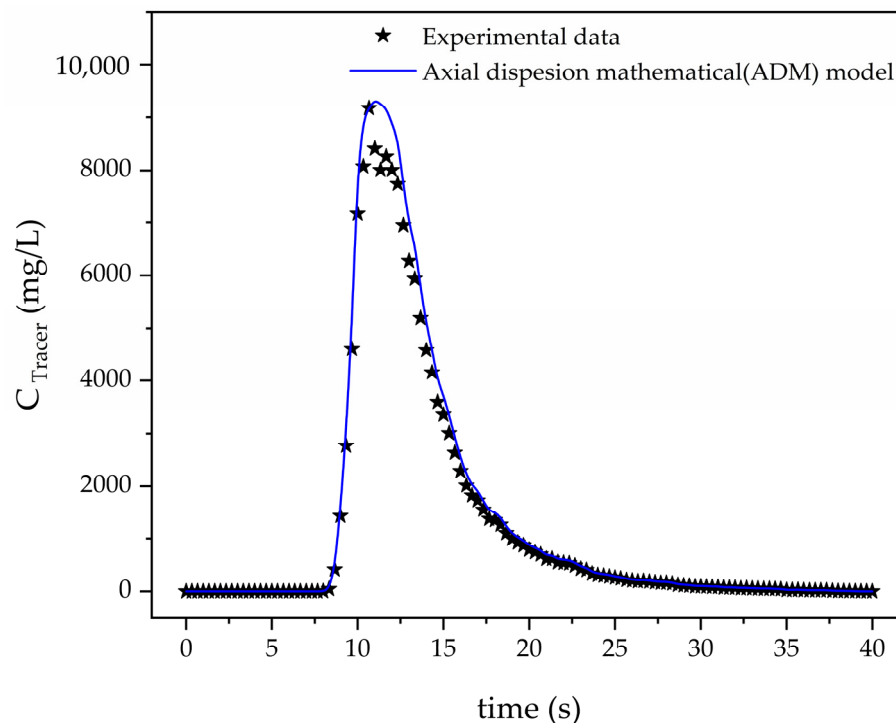


**Figure 2.** Tracer concentration curve obtained in the FBR via the ADM model at a flow rate of 1.0 L/min.

Toward completing the parameters of the ADM model, the axial dispersion coefficient ( $D_{ax} = 5 \text{ cm}^2/\text{s}$ ) was determined by using Equation (21) in accordance with reference [31], at a volumetric flow rate ( $Q$ ) of 1 L/min, a reactor longitude ( $l$ ) of 20 cm, and a linear velocity ( $u$ ) of 9.5 cm/s. The computed axial dispersion coefficient demonstrates a low deviation from the ideal plug-flow pattern ( $D_{ax} = 0 \text{ cm}^2/\text{s}$ ) since the value is less than  $50 \text{ cm}^2/\text{s}$ , which agrees with that given in reference [17].

$$\frac{\sigma^2}{t_m^2} = 2 \left( \frac{D_{ax}}{ul} \right) - 2 \left( \frac{D_{ax}}{ul} \right)^2 \left[ 1 - \exp \left( -\frac{ul}{D_{ax}} \right) \right] \quad (21)$$

### 3.2. Kinetic Reaction of 2-CP

Upon performing the electrochemical degradation of 2-CP and analyzing the samples via UHPLC each hour during the reaction time (4 h), the experimental data are plotted in Figure 3. The behavior exhibited in Figure 3 suggests that the electrochemical degradation of 2-CP follows a pseudo-first-order kinetic model (see Equation (6)). Additionally, the curve shape in Figure 3 suggests a large amount of hydroxyl radicals ( $\text{OH}^\bullet$ ), which are produced on the BDD anode surface via the oxidation of the water as reported in reference [11]. Complete data from the UHPLC analysis can be consulted in the Supplementary Material.

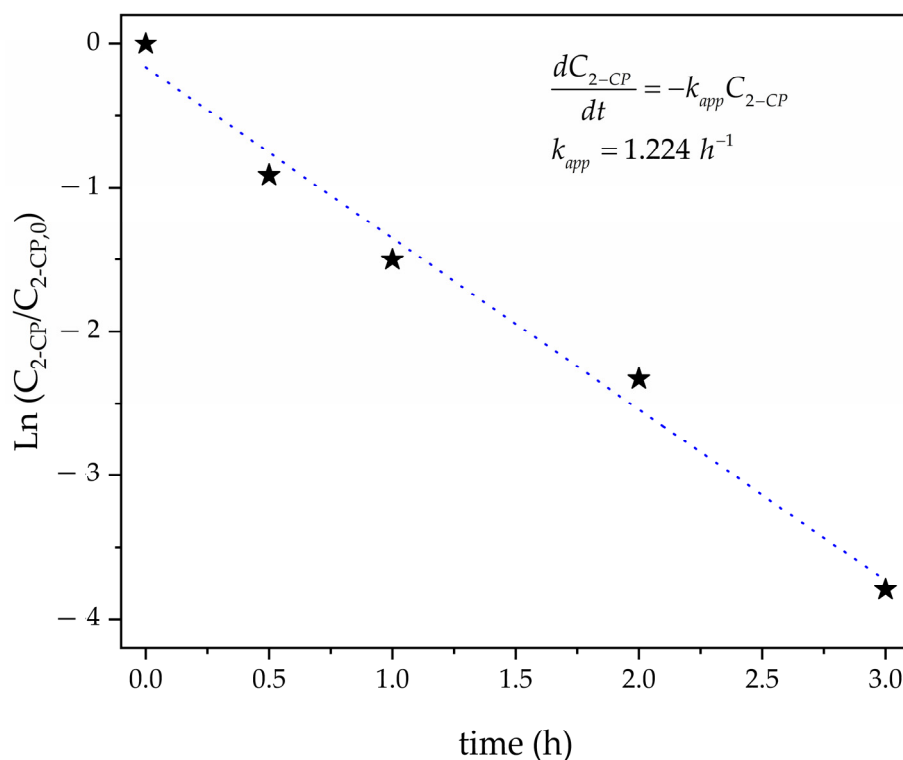


**Figure 3.** Kinetic reaction model of the electrochemical degradation of 2-CP at a flow rate of 1.0 L/min, an initial pH of 7.3, a current density of 0.14 A/cm<sup>2</sup>, and a temperature of 25 °C.

The apparent kinetic constant ( $k_{app} = 1.224 \text{ h}^{-1}$ ) was determined by fitting a linear regression of  $\text{Ln}(C_{2-CP}/C_{2-CP,0})$  versus time with a determination coefficient ( $R^2$ ) of 0.9850 based on the integral method according to reference [32].

### 3.3. Modeling of the Complete Degradation Efficiency of 2-CP

The degradation efficiency of 2-CP ( $\eta$ , see Equation (9)) was employed to validate the parametric mathematical model (ADM model) developed in this manuscript with the experimental data and compared with a previous work by the author [18]. In Figure 4a, the major change on  $\eta$  occurs at approximately 2 h. Additionally, Figure 4a presents an asymptotic behavior that tends to 100% degradation efficiency. This behavior was expected because the  $\text{OH}^\bullet$  generated on the BDD anode surface is constant and sufficient to oxidize the 2-CP. Moreover, the parametric mathematical model proposed here predicts the concentration abatement of 2-CP due to the interaction of 2-CP with  $\text{OH}^\bullet$  (according to Equation (1)) in favor of an instantaneous reaction on the BDD anode. Upon this, the 2-CP concentration depletes rapidly to zero because the reaction rate is controlled by mass transfer. Hence, the 2-CP from the bulk solution goes rapidly to the BDD anode surface according to [22]. Moreover, as the mass transport resistance from the bulk solution towards the BDD anode surface here is low, a small diffusion layer thickness at the electrode interface is present [33,34].

Figure 4b shows the distribution of experimental versus predicted values of the degradation efficiency of 2-CP; a satisfactory correlation between the experimental and predicted values of the degradation efficiency of 2-CP is depicted.

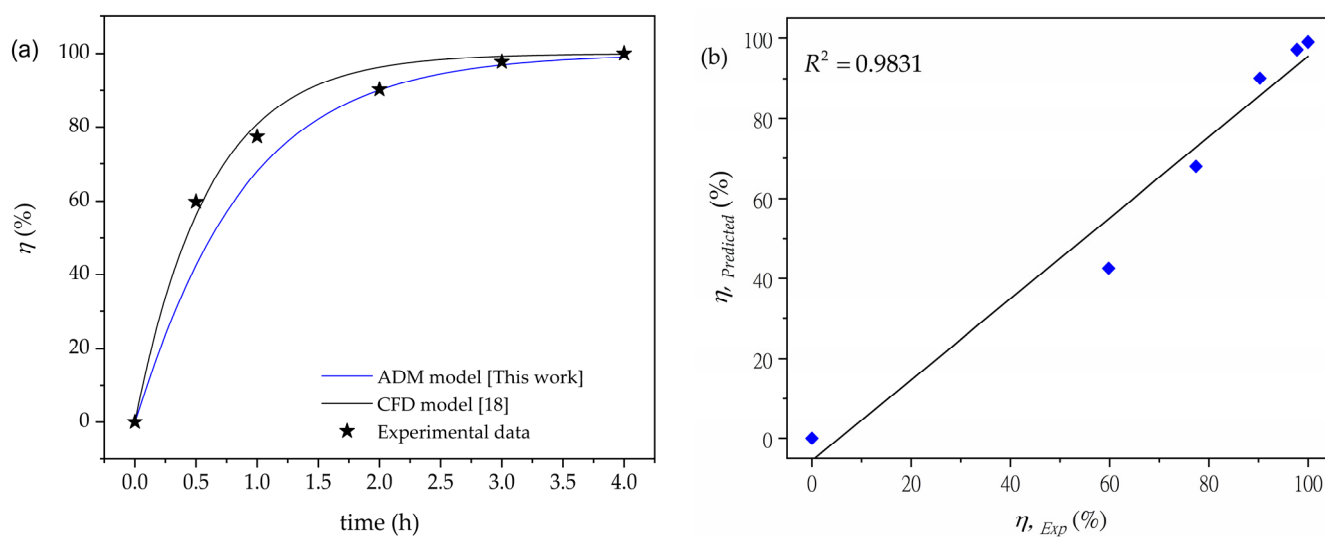


**Figure 4.** (a) Degradation efficiency of 2-CP. (b) Parity diagram of the degradation efficiency of 2-CP.

The degradation efficiency of 2-CP estimated using the parametric mathematical model (ADM model) was 99.06%, whereas the experimental concentration reached was 99.99% (a relative error of 0.93%). This confirmed the predictive capacity of the parametric mathematical modeling, as well as the efficiency of the applied electro-oxidation process. It is worth mentioning that the computer time required to solve the parametric mathematical model was 8 s, whereas the computer time required to solve the model in reference [18] was 42 days. Hence, this indicates that the model developed in this research is appropriate to well describe the electrochemical degradation process of 2-CP, could be applied relatively easily to further applications, e.g., scaling-up purposes or modeling the electrochemical degradation of any emerging contaminant in the same reactor, and is appropriated to design control system strategies such as linear control, non-linear control, predictive model control, and plantwide control, among others.

Toward verifying the accuracy of the parametric mathematical model of the degradation efficiency of 2-CP with the experimental data, different index performances were tested (see Table 2). The model prediction is in very good agreement with the experimental data because the determination coefficient value ( $R^2$ ) is close to 1.0, which is cataloged as an excellent model fitting since  $R^2$  is greater than 0.9 [35]. Additionally, the reduced root-mean-square error value (RMSE of 0.174) is close to 0, indicating that the ADM model agrees very well with the experimental data [36]. The value of the mean square error (MSE = 0.0307) indicates that the degradation efficiency of 2-CP predicted by the ADM model fits very well with the experimental data of the degradation efficiency since the MSE value is close to 0 [37,38].

**Table 2.** Regression quality measures of the ADM model with experimental data.

Index Performance	Value	Remark
$R^2$	0.9831	Excellent model fit
MSE	0.0307	Very good model fit
RMSE	0.1754	Very good model fit

### 3.4. Total Operating Cost

The total energy consumption and operating cost were computed according to Section 2.4.5. Thus, the pilot electrochemical plant consumes 1.735 kW h when treating 2.5 L of 2-CP solution. This corresponds to a total operating cost of USD 0.359 for the 2.5 L treated or 0.143 USD/L. It is worth mentioning that in this research, the cost of the

electrolyte was USD 0.085. However, all the above results disclose the potential of the used electrochemical plant to remove emerging contaminants such as 2-CP from wastewater.

Regarding the degradation efficiency of 2-CP, the principal reports are displayed in Table 3. It is difficult to establish a comparison on the degradation efficiency of 2-CP between the literature and this work when the processes were performed at different concentrations. Nevertheless, it can be noted that only two works [39,40] achieve similar efficiency to this research; however, the volumes treated in those studies were less than the volume treated in the current work. Additionally, in this work, the applied current density is higher than in other studies because the anode and cathode were made from the same material. As the BDD anode is considered a semiconductor, a higher current density than that reference in [39] (where stainless-steel cathode was used) is required. Although the concentrations used in the studies reported in Table 3 were higher than the concentration ( $1 \text{ mol/m}^3$ ) used here, this work is highlighted as a suitable electrochemical plant for the treatment of wastewater containing 2-CP with a treated volume of 2.5 L.

**Table 3.** Summary of the electrochemical degradation efficiency of 2-CP.

Current Density (mA/cm <sup>2</sup> )	$V_{treated}$ (L)	A (cm <sup>2</sup> )	C (mol/m <sup>3</sup> )	Electrodes		$\eta$ (%)		Reference
				Anode	Cathode	Exp.	Pred.	
140.0	2.50	32	1.00	BDD	BDD	99.99	99.06	[This work]
100.0	0.025	2	5.00	Carbon fiber	-	98.00	-	[40]
32.7	0.030	14	10.00	BDD	-	83.60	-	[41]
90.0	1.00	70	15.56	BDD	Stainless steel	100.00	-	[39]
16.0	0.30	-	4.70	Ti/SnO <sub>2</sub>	-	50.00	-	[42]
33.0	0.07	9	1.56	Graphite felts	Pt	58.91	-	[43]

### 3.5. Future Works

The mathematical model proposed here could ensure high performance and autonomy and guarantees the optimal operation of electrochemical plants through the maximization of the removal efficiency of contaminants and the minimization of energy consumption. Therefore, advanced optimization methods and advanced control strategies must be developed. To accomplish these tasks, real-time supervisor systems, machine learning algorithms, model predictive control strategies, and plantwide control strategies must be implemented in electrochemical plants, which could consider as key variables the initial pH, current density, electrode potential, volumetric flow rate, conductivity, residence time, and temperature. Additionally, to make electrochemical plants a preferable technology, they must be environmentally sustainable and technoeconomically attractive. This implies making the electrochemical plants scalable from a low-cost perspective and performing life cycle assessment studies. Finally, these challenges regarding techno-economics must be achieved through multidisciplinary work in which the direct participation of specialists in electrochemical, chemical engineering, energy, artificial intelligence, economy, and environmental engineering is needed.

## 4. Conclusions

The parametric mathematical model of the degradation efficiency of 2-CP in a pilot electrochemical plant under batch recirculation mode has high reproducibility since all index performances ( $R^2$ , MSE, and RMSE) classify the data prediction as very good model fitting concerning the experimental data. Additionally, the numerical solution strategy followed in this research to solve a partial differential equation (PDE) with an ordinary differential equation (ODE) was successful because the computing time solution was very short (8 s). Furthermore, the model established here is reliable for future electrochemical treatments when the electrochemical process is limited by mass transport and for scaling-up the same flow-by reactor.

**Supplementary Materials:** The following supporting information can be downloaded at: <https://www.mdpi.com/article/10.3390/w15244276/s1>, Table S1: Results of UHPLC analysis.

**Author Contributions:** Conceptualization, R.N. and A.R.-M.; methodology, A.R.-M.; software, M.E.C. and L.Z.; validation, G.R.-H., E.P.-R. and A.R.-M.; formal analysis, A.R.-M.; investigation, G.R.-H. and A.R.-M.; resources, A.R.-M., E.E.R.-G. and E.P.-R.; data curation, R.N., H.P.-P., E.E.R.-G. and A.R.-M.; writing—original draft preparation, A.R.-M.; writing—review and editing, R.N., A.R.-M., M.E.C., L.Z., E.E.R.-G., H.P.-P. and E.P.-R.; visualization, E.P.-R., R.N. and A.R.-M.; supervision, A.R.-M.; project administration, A.R.-M.; funding acquisition, A.R.-M. and E.P.-R. All authors have read and agreed to the published version of the manuscript.

**Funding:** This research received no external funding.

**Data Availability Statement:** All data that support the results of this manuscript can be found in the Supplementary Materials file.

**Acknowledgments:** Authors (A.R.-M., E.P.-R., R.N., M.E.C., L.Z., H.P.-P. and E.E.R.-G.) are grateful to CONAHCyT for the financial support through the Investigators National System (SNII) program.

**Conflicts of Interest:** The authors declare no conflict of interest.

### Appendix A

In this section, some details about the derivation of the axial dispersion mathematical model for the flow-by reactor (Appendix A.1, see Figure A1a) and the continuous stirred tank (CST) model for the reservoir tank (Appendix A.2, see Figure A1b) are presented.

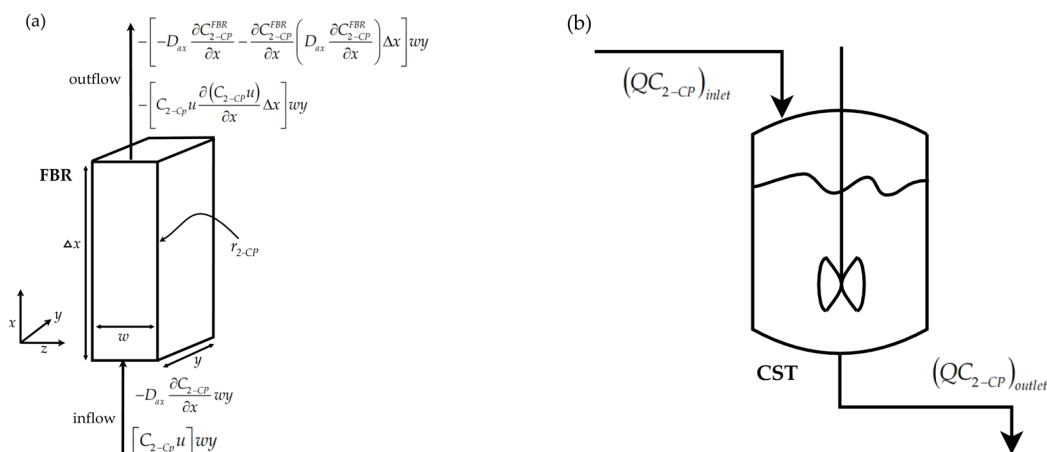


**Figure A1.** (a) Volume element of the FBR for shell mass balance. (b) Diagram of the CST for macroscopic mass balance.

#### Appendix A.1. Axial Dispersion Mathematical Model for the Flow-By Reactor

$$\left( \begin{matrix} \text{Rate of} \\ \text{acumulation} \\ \text{of 2-CP} \end{matrix} \right) = \left( \begin{matrix} \text{Rate of inflow} \\ \text{of 2-CP} \end{matrix} \right) \Big|_x - \left( \begin{matrix} \text{Rate of outflow} \\ \text{of 2-CP} \end{matrix} \right) \Big|_{x+\Delta x} \pm \left( \begin{matrix} \text{Electrochemical} \\ \text{reaction rate} \\ \text{of 2-CP} \end{matrix} \right) \quad (A1)$$

$$wy\Delta x \frac{\partial C_{2-CP}^{FBR}}{\partial t} = -D_{ax} \frac{\partial C_{2-CP}^{FBR}}{\partial x} wy - \left[ -D_{ax} \frac{\partial C_{2-CP}^{FBR}}{\partial x} - \frac{\partial C_{2-CP}^{FBR}}{\partial x} \left( D_{ax} \frac{\partial C_{2-CP}^{FBR}}{\partial x} \right) \Delta x \right] wy + \left[ C_{2-CP}^{FBR} \cdot u \right] wy - \left[ C_{2-CP}^{FBR} \cdot u \frac{\partial (C_{2-CP}^{FBR} \cdot u)}{\partial x} \right] wy + r_{2-CP} wy \Delta x \quad (A2)$$

Reordering Equation (A2), we can obtain Equation (A3):

$$wy\Delta x \frac{\partial C_{2-CP}^{FBR}}{\partial t} = \frac{\partial}{\partial x} \left( D_{ax} \frac{\partial C_{2-CP}^{FBR}}{\partial x} \right) wy\Delta x - \frac{\partial (C_{2-CP}^{FBR} \cdot u)}{\partial x} \Delta x wy + r_{2-CP} wy \Delta x \quad (A3)$$

Dividing Equation (A3) by the volume element ( $w y \Delta x$ ) and considering that  $D_{ax}$  is constant, Equation (A3) reduces to:

$$\frac{\partial C_{2-CP}^{FBR}}{\partial t} = D_{ax} \frac{\partial^2 C_{2-CP}^{FBR}}{\partial x^2} - \frac{\partial (C_{2-CP}^{FBR} \cdot u)}{\partial x} + r_{2-CP} \quad (A4)$$

$$At x = 0 \quad D_{ax} \frac{\partial^2 C_{2-CP}^{FBR}}{\partial x^2} = u \cdot C_{2-CP, 0} \quad \forall t > 0 \quad (A5)$$

$$At x = \uparrow \quad -D_{ax} \frac{\partial^2 C_{2-CP}^{FBR}}{\partial x^2} = 0 \quad \forall t > 0 \quad (A6)$$

$$At t = 0 \quad C_{2-CP}^{FBR} = C_{2-CP, 0} \quad (A7)$$

#### Appendix A.2. Continuous Stirred Tank (CST) Model for the Reservoir Tank

$$\left[ \begin{array}{c} \text{Rate of accumulation} \\ \text{of 2-CP} \end{array} \right] = \left[ \begin{array}{c} \text{Rate of inflow} \\ \text{of 2-CP} \end{array} \right] - \left[ \begin{array}{c} \text{Rate of outflow} \\ \text{of 2-CP} \end{array} \right] \quad (A8)$$

$$\frac{dm_{2-CP}}{dt} = (QC_{2-CP}^{CST})_{inlet} - (QC_{2-CP}^{CST})_{outlet} \quad (A9)$$

Considering that  $C_{2-CP}^{CST} = m_{2-CP}/V_T$ , we can reorder Equation (A9) as:

$$\frac{d(V_T C_{2-CP}^{CST})}{dt} = Q_{inlet} C_{2-CP}^{FBR} - Q_{outlet} C_{2-CP}^{CST} \quad (A10)$$

Assuming that the volume  $V_T$  is constant and the volumetric flow rates of the inflow and outflow streams are the same ( $Q_{inlet} = Q_{outlet} = Q$ ), Equation (A10) reduces to:

$$\frac{dC_{2-CP}^{CST}}{dt} = \frac{Q}{V_T} (C_{2-CP}^{FBR} - C_{2-CP}^{CST}) \quad (A11)$$

$$At t = 0 \quad C_{2-CP}^{CST} = C_{2-CP, 0} \quad (A12)$$

## References

- Valadez-Renteria, E.; Barrera-Rendon, E.; Oliva, J.; Rodriguez-Gonzalez, V. Flexible CuS/TiO<sub>2</sub> Based Composites Made with Recycled Bags and Polystyrene for the Efficient Removal of the 4-CP Pesticide from Drinking Water. *Sep. Purif. Technol.* **2021**, *270*, 118821. [CrossRef]
- Xu, J.; Lv, X.; Li, J.; Li, Y.; Shen, L.; Zhou, H.; Xu, X. Simultaneous Adsorption and Dechlorination of 2,4-Dichlorophenol by Pd/Fe Nanoparticles with Multi-Walled Carbon Nanotube Support. *J. Hazard. Mater.* **2012**, *225–226*, 36–45. [CrossRef]
- Ahmaruzzaman, M. Adsorption of Phenolic Compounds on Low-Cost Adsorbents: A Review. *Adv. Colloid Interface Sci.* **2008**, *143*, 48–67. [CrossRef]
- Janda, V.; Ávecov, M. By-Products in Drinking Water Disinfection. *Chemické Listy* **2000**, *94*. Available online: <http://www.chemicke-listy.cz/ojs3/index.php/chemicke-listy/article/view/2477> (accessed on 29 October 2023).
- Machado, L.M.M.; Lütke, S.F.; Perondi, D.; Godinho, M.; Oliveira, M.L.S.; Collazzo, G.C.; Dotto, G.L. Treatment of Effluents Containing 2-Chlorophenol by Adsorption onto Chemically and Physically Activated Biochars. *J. Environ. Chem. Eng.* **2020**, *8*, 104473. [CrossRef]
- Barbeni, M.; Minero, C.; Pelizzetti, E.; Borgarello, E.; Serpone, N. Chemical Degradation of Chlorophenols with Fenton's Reagent (Fe<sup>2+</sup> + H<sub>2</sub>O<sub>2</sub>). *Chemosphere* **1987**, *16*, 2225–2237. [CrossRef]
- Lin, Y.-H.; Wu, C.-H. Kinetics of the Biodegradation of Phenol and 2-Chlorophenol in a Fixed Biofilm Reactor Using a Dewatered Sludge-Fly Ash Composite Ceramic Particle as a Supporting Medium. *Desalination Water Treat.* **2019**, *157*, 39–52. [CrossRef]
- Rao, N.N.; Dubey, A.K.; Mohanty, S.; Khare, P.; Jain, R.; Kaul, S.N. Photocatalytic Degradation of 2-Chlorophenol: A Study of Kinetics, Intermediates and Biodegradability. *J. Hazard. Mater.* **2003**, *101*, 301–314. [CrossRef]
- Muddemann, T.; Haupt, D.; Sievers, M.; Kunz, U. Electrochemical Reactors for Wastewater Treatment. *ChemBioEng Rev.* **2019**, *6*, 142–156. [CrossRef]

10. Silva, B.S.; Ribeiro, M.C.B.; Ramos, B.; de Castro Peixoto, A.L. Removal of Amoxicillin from Processing Wastewater by Ozonation and UV-Aided Ozonation: Kinetic and Economic Comparative Study. *Water* **2022**, *14*, 3198. [[CrossRef](#)]
11. Bany Abdelnabi, A.A.; Al Theeb, N.; Almomani, M.A.; Ghanem, H.; Rosiwal, S.M. Effect of Electrode Parameters in the Electro-Production of Reactive Oxidizing Species via Boron-Doped Diamond under Batch Mode. *Water Environ. Res.* **2022**, *94*, e10830. [[CrossRef](#)]
12. Legrini, O.; Oliveros, E.; Braun, A.M. Photochemical Processes for Water Treatment. *Chem. Rev.* **1993**, *93*, 671–698. [[CrossRef](#)]
13. Yu, S.; Liu, S.; Jiang, X.; Yang, N. Recent Advances on Electrochemistry of Diamond Related Materials. *Carbon* **2022**, *200*, 517–542. [[CrossRef](#)]
14. Rivero, E.P.; Rodríguez, F.A.; Cruz-Díaz, M.R.; González, I. Reactive Diffusion Migration Layer and Mass Transfer Wall Function to Model Active Chlorine Generation in a Filter Press Type Electrochemical Reactor for Organic Pollutant Degradation. *Chem. Eng. Res. Des.* **2018**, *138*, 533–545. [[CrossRef](#)]
15. Rivera, F.F.; Castañeda, L.; Hidalgo, P.E.; Orozco, G. Study of Hydrodynamics at Asahi™ Prototype Electrochemical Flow Reactor, Using Computational Fluid Dynamics and Experimental Characterization Techniques. *Electrochim. Acta* **2017**, *245*, 107–117. [[CrossRef](#)]
16. Rivera, F.F.; Pérez, T.; Castañeda, L.F.; Nava, J.L. Mathematical Modeling and Simulation of Electrochemical Reactors: A Critical Review. *Chem. Eng. Sci.* **2021**, *239*, 116622. [[CrossRef](#)]
17. Levenspiel, O. The Dispersion Model. In *Tracer Technology: Modeling the Flow of Fluids*; Levenspiel, O., Ed.; Springer: New York, NY, USA, 2012; pp. 47–70, ISBN 978-1-4419-8074-8.
18. Regalado-Méndez, A.; Cruz-López, A.; Mentado-Morales, J.; Cordero, M.E.; Zárate, L.G.; Cruz-Díaz, M.R.; Fontana, G.; Peralta-Reyes, E. Mathematical Modeling of the Electrochemical Degradation of 2-Chlorophenol Using an Electrochemical Flow Reactor Equipped with BDD Electrodes. *J. Flow Chem.* **2019**, *9*, 59–71. [[CrossRef](#)]
19. Palma-Goyes, R.E.; Sosa-Rodríguez, F.S.; Rivera, F.F.; Vazquez-Arenas, J. Modeling the Sulfamethoxazole Degradation by Active Chlorine in a Flow Electrochemical Reactor. *Environ. Sci. Pollut. Res.* **2021**, *29*, 42201–42214. [[CrossRef](#)] [[PubMed](#)]
20. Castañeda Ulloa, L.F.; Cornejo, O.M.; Nava, J.L. Modeling of the Electro-Peroxone Process for the Degradation of Orange Reactive 16 Dye. *ECS Trans.* **2018**, *86*, 129–138. [[CrossRef](#)]
21. Zier, T.; Bouafia, S.; Rechidi, Y.; Chabani, M. Hydrodynamics Modeling and Electrochemical Performance of a Lab-Scale Single-Channel Cell through Residence Time Distribution and Kinetic Studies. *Desalination Water Treat.* **2022**, *279*, 187–194. [[CrossRef](#)]
22. Rivera, F.F.; Rodríguez, F.A.; Rivero, E.P.; Cruz-Díaz, M.R. Parametric Mathematical Modelling of Cristal Violet Dye Electrochemical Oxidation Using a Flow Electrochemical Reactor with BDD and DSA Anodes in Sulfate Media. *Int. J. Chem. React. Eng.* **2018**, *16*, 20170116. [[CrossRef](#)]
23. Cruz-Díaz, M.R.; Rivero, E.P.; Rodríguez, F.A.; Domínguez-Bautista, R. Experimental Study and Mathematical Modeling of the Electrochemical Degradation of Dyeing Wastewaters in Presence of Chloride Ion with Dimensional Stable Anodes (DSA) of Expanded Meshes in a FM01-LC Reactor. *Electrochim. Acta* **2018**, *260*, 726–737. [[CrossRef](#)]
24. Regalado-Méndez, A.; Mentado-Morales, J.; Vázquez, C.E.; Martínez-Villa, G.; Cordero, M.E.; Zárate, L.G.; Skogestad, S.; Peralta-Reyes, E. Modeling and Hydraulic Characterization of a Filter-Press-Type Electrochemical Reactor by Using Residence Time Distribution Analysis and Hydraulic Indices. *Int. J. Chem. React. Eng.* **2018**, *16*, 20170210. [[CrossRef](#)]
25. Peralta-Reyes, E.; Natividad, R.; Castellanos, M.; Mentado-Morales, J.; Cordero, M.E.; Amado-Piña, D.; Regalado-Méndez, A. Electro-Oxidation of 2-Chlorophenol with BDD Electrodes in a Continuous Flow Electrochemical Reactor. *J. Flow Chem.* **2020**, *10*, 437–447. [[CrossRef](#)]
26. Pérez, T.; León, M.I.; Nava, J.L. Numerical Simulation of Current Distribution along the Boron-Doped Diamond Anode of a Filter-Press-Type FM01-LC Reactor during the Oxidation of Water. *J. Electroanal. Chem.* **2013**, *707*, 1–6. [[CrossRef](#)]
27. Danckwerts, P.V. Continuous Flow Systems: Distribution of Residence Times. *Chem. Eng. Sci.* **1953**, *2*, 1–13. [[CrossRef](#)]
28. Kim, S.; Kim, Y.K. Apparent Desorption Kinetics of Phenol in Organic Solvents from Spent Activated Carbon Saturated with Phenol. *Chem. Eng. J.* **2004**, *98*, 237–243. [[CrossRef](#)]
29. Karunasingha, D.S.K. Root Mean Square Error or Mean Absolute Error? Use Their Ratio as Well. *Inf. Sci.* **2022**, *585*, 609–629. [[CrossRef](#)]
30. Guisan, A.; Thuiller, W.; Zimmermann, N.E. Measuring Model Accuracy: Which Metrics to Use? In *Habitat Suitability and Distribution Models*; Cambridge University Press: Cambridge, UK, 2017; pp. 241–269.
31. Levenspiel, O. The Tracer Method. *Fluid Mech. Its Appl.* **2012**, *96*, 1–3. [[CrossRef](#)]
32. Fogler, H.S. *Elements of Chemical Reaction Engineering*, 6th ed.; Pearson Education Limited: London, UK, 2022; ISBN 1-292-41666-1.
33. Fitch, A.; Balderas-Hernandez, P.; Ibanez, J.G. Electrochemical Technologies Combined with Physical, Biological, and Chemical Processes for the Treatment of Pollutants and Wastes: A Review. *J. Environ. Chem. Eng.* **2022**, *10*, 107810. [[CrossRef](#)]
34. Abbasi, P.; Bahrami Moghadam, E. Electrochemical Degradation of Ciprofloxacin from Water: Modeling and Prediction Using ANN and LSSVM. *Phys. Chem. Earth Parts A/B/C* **2023**, *132*, 103509. [[CrossRef](#)]
35. Montgomery, D.C. *Design and Analysis of Experiments*, 2nd ed.; Wiley: New York, NY, USA, 1984.
36. Mequanient, M.B.; Kebede, H.H. Simulation of Sediment Yield and Evaluation of Best Management Practices in Azuari Watershed, Upper Blue Nile Basin. *H2Open J.* **2023**, *6*, 493–506. [[CrossRef](#)]

37. Tyagi, K.; Rane, C.; Harshvardhan; Manry, M. Regression Analysis. In *Artificial Intelligence and Machine Learning for EDGE Computing*; Academic Press: Cambridge, MA, USA, 2022; pp. 53–63. [[CrossRef](#)]
38. Wang, X.; Yang, J.; Wang, F.; Xu, N.; Li, P.; Wang, A. Numerical Modeling of the Dispersion Characteristics of Pollutants in the Confluence Area of an Asymmetrical River. *Water* **2023**, *15*, 3766. [[CrossRef](#)]
39. Vallejo, M.; San Román, M.F.; Ortiz, I. Quantitative Assessment of the Formation of Polychlorinated Derivatives, PCDD/Fs, in the Electrochemical Oxidation of 2-Chlorophenol as Function of the Electrolyte Type. *Environ. Sci. Technol.* **2013**, *47*, 12400–12408. [[CrossRef](#)]
40. Yoon, J.H.; Jeong, E.D.; Shim, Y.B.; Won, M.S. Anodic Degradation of Toxic Aromatic Compound in the Flow Through Cell with Carbon Fiber Electrode. *Key Eng. Mater.* **2005**, *277–279*, 445–449. [[CrossRef](#)]
41. Yoon, J.-H.; Shim, Y.-B.; Lee, B.-S.; Choi, S.-Y.; Won, M.-S. Electrochemical Degradation of Phenol and 2-Chlorophenol Using Pt/Ti and Boron-Doped Diamond Electrodes. *Bull. Korean Chem. Soc.* **2012**, *33*, 2274–2278. [[CrossRef](#)]
42. Polcaro, A.M.; Palmas, S.; Renoldi, F.; Mascia, M. On the Performance of Ti/SnO<sub>2</sub> and Ti/PbO<sub>2</sub> Anodes in Electrochemical Degradation of 2-Chlorophenol for Wastewater Treatment. *J. Appl. Electrochem.* **1999**, *29*, 147–151. [[CrossRef](#)]
43. Yang, K.; Zhao, Y.; Zhou, X.; Wang, Q.; Pedersen, T.H.; Jia, Z.; Cabrera, J.; Ji, M. “Self-Degradation” of 2-Chlorophenol in a Sequential Cathode-Anode Cascade Mode Bioelectrochemical System. *Water Res.* **2021**, *206*, 117740. [[CrossRef](#)]

**Disclaimer/Publisher’s Note:** The statements, opinions and data contained in all publications are solely those of the individual author(s) and contributor(s) and not of MDPI and/or the editor(s). MDPI and/or the editor(s) disclaim responsibility for any injury to people or property resulting from any ideas, methods, instructions or products referred to in the content.